Soils and Foundations 2014;54(2):168–175

The Japanese Geotechnical Society

Soils and Foundations

www.sciencedirect.com
journal homepage: www.elsevier.com/locate/sandf

Uplift tests of jet mixing anchor pile

Hai-yong Xu, Long-zhu Chen*, Jian-liang Deng

Institute of Engineering Safety & Disaster Prevention, Shanghai Jiao Tong University, Shanghai 200240, China

Received 5 July 2012; received in revised form 12 October 2013; accepted 14 November 2013
Available online 24 March 2014

Abstract

The jet mixing anchor pile is a new kind of supporting technology for foundation pit engineering in soft clay. The engineering features of jet mixing anchor pile as well as the difference between it and normal anchor bolt are introduced. The uplift tests of 4 jet mixing anchor piles are presented in detail to obtain the ultimate bearing capacity and load–deformation relationship of the piles. Load-transfer analysis, which is rarely applied in the analysis of uplift piles, is carried out on the piles with a hyperbolic calculation model. The load transfer method focuses on the interface between pile and soil, with which the non-linear behavior, the bearing capacity and the engineering features of the anchor piles can be fully studied. The calculated load–displacement curves of the piles have close agreement with that of the pullout tests, indicating that the proposed analytical solution is reasonable and feasible in predicting the bearing capacity of the piles. Thus, with this study, the supporting stiffness of the anchor pile can be predicted in the design stage of the foundation pit engineering, which is very important and meaningful in practical engineering. The decay curve of shear stress of soil surrounding the pile is derived with the load-transfer method, through which the minimum transverse space of each two piles can be decided against the pile group effect. Engineers can optimize the length and spacing of group piles through this.

Keywords: Jet mixing anchor pile; Uplift test; Load-transfer analysis; Pile group effect

1. Introduction

The jet mixing anchor pile is a new kind of supporting technology for foundation pits and slopes. Besides having some similar characteristics to soil anchors (Miyata et al., 2009), it has some extra engineering features and advantages. The jet mixing anchor pile is good in deformation control and capable of maintaining the stability of the whole supporting structure. It can be applied to excavations in much the same manner as a multi-anchor wall (Richard et al., 2011) and can meet the strict demand for deformation. Compared with traditional supporting technology, it is much lower in cost and more environment-friendly. Jet mixing anchor piles and struts are both used in a long strip excavation in the city of Wuhan, China. It is reported that for each section of 26 m in length along the exaction, 7 days was requires for excavation when using anchor piles, 2 days less than that required for struts. On the other hand, though concrete struts need to be removed by explosive demolition, the strands in the anchor piles can be recoverable for recycling use, which reduces the cost by about

*Corresponding author.
E-mail addresses: seamanxhy@sjtu.edu.cn, xhy85@yahoo.com.cn (H.-y. Xu), lzchen@sjtu.edu.cn (L.-z. Chen), dengjianliang@sjtu.edu.cn (J.-l. Deng).
Peer review under responsibility of The Japanese Geotechnical Society.

Production and hosting by Elsevier

http://dx.doi.org/10.1016/j.sandf.2014.02.008

20%. It has been applied to more than 120 excavation projects and brought about significant economic and social benefit (Liu, 2011), which are proof of the feasibility and maturity of this technology. The deepest foundation pit supported by jet mixing anchor pile is 27 m in depth.

A series of pullout tests on jet mixing anchor pile were conducted in Jingjiang, in the Jiangsu province of China. The soil layer properties, process and results of the tests are presented in this paper. The load-transfer method is that commonly used for calculations of compression piles (Hirayama, 1990; Cem et al., 2012) but has not yet been widely accepted in uplift piles. Even in the methods currently used (Reddy et al., 1998; Shubhra et al., 2007)), the application of the load transfer method is not simplified enough. The proposed method in this manuscript is simple with fewer parameters but a clear derivation, and the results are satisfactory. The hyperbolic load–displacement model, which is widely used in the analysis of compression piles and soil anchors, is applied to derive the implicit relationship between the tension load and the deformation of the test piles. The decay mode of the shear stress of the soil surrounding the pile is obtained based on the load-transfer analysis, through which the minimum transverse space of each two piles can be decided against the pile group effect.

2. Definition and engineering features of jet mixing anchor pile

Pile foundation engineering is widely studied all over the world (Pastaskorn et al., 2011; Kiyoshi et al., 2011). Compared with normal anchors, Jet mixing anchor piles are more like piles. They are made of steel strands and cemented soil by swing-injected agitation and are used to reinforce and support foundation soils and slopes. The difference between typical jet mixing anchor piles and normal anchors is shown in Fig. 1.

Because the diameter of the jet mixing anchor pile (400–1000 mm) is much larger than that of normal anchors (less than 100 mm), the contact area and the frictional resistance between the pile and soil is also larger. The cemented soil is infused into the hole by high pressure jet grouting whereas normal anchors are made by low-pressure grouting. Together with the fix function of the anchor plates at the bottom part of the steel strand, the bond between the cement grout and steel strand is very strong. These engineering features make it possible for anchor piles to be used in soft soil, especially in silt clay, where normal anchors are not recommended by engineering specifications.

Typical jet mixing anchor piles can be divided into two sections: the free section and anchorage section. As shown in Fig. 1, the steel strand of the free section is not bonded with the cement grout so that it can be pre-stressed in posterior construction.

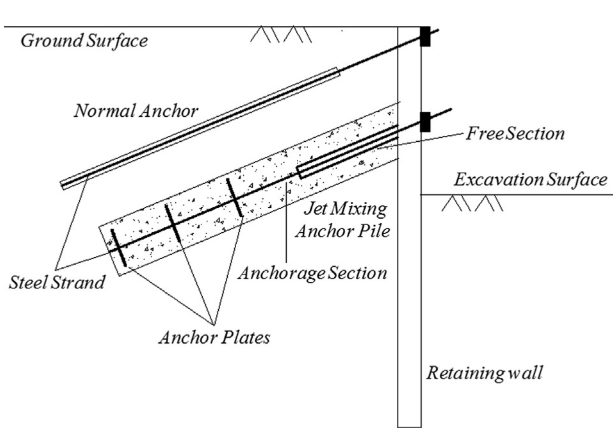

Fig. 1. Difference between jet mixing anchor pile and normal anchor.

3. Uplift tests

The Kaixuan project is located in the city of Jingjiang, Jiangsu province of China. Uplift tests were carried out on 4 jet mixing anchor piles in order to investigate the ultimate bearing capacity and load–deformation relationship of the piles of the project. All the 4 test piles are divided into two groups by length, see Table 1. The steel strand is composed of 3ϕ 15.2 mm steel bars. The schematic diagram and photo of the test equipment are shown in Figs. 2 and 3.

The failure criterion and termination condition of the test are as follows:

(1) The anchor pile is pulled out from the foundation soil.
(2) The displacement of the head of the anchor pile under one load level is two times than that under the nearest former level.
(3) The anchor pile is broken under the tension load.

The pile test is ended if any of the former 3 condition happens. It was found that the limitations of the tension load of the tests was about 500 kN with a series of load and unload process.

All of the uplift tests were carried out in the second layer of the foundation soil, see Fig. 4. The soil is a mucky silt clay. The parameters of the soil profile are shown in Table 2.

The load–unload curves of the 4 test piles are shown in Fig. 8(a)–(d), where (a) and (b) are from group 1. Several conclusions can be made from the figures. The final displacements of the 2 test piles from each group were in good agreement, which indicates the tests are reliable. Since there is no obvious yielding in the curves before the axial load reaches 400 kN, it can be deduced that the ultimate bearing capacity of the piles is satisfactory. Jet mixing anchor piles can be applied

Table 1
Parameters of the test piles.

Group number	Whole length (m)	Free section length (m)	Anchorage section length (m)	Diameter (mm)
1	18	6	12	600
2	24	11	13	600

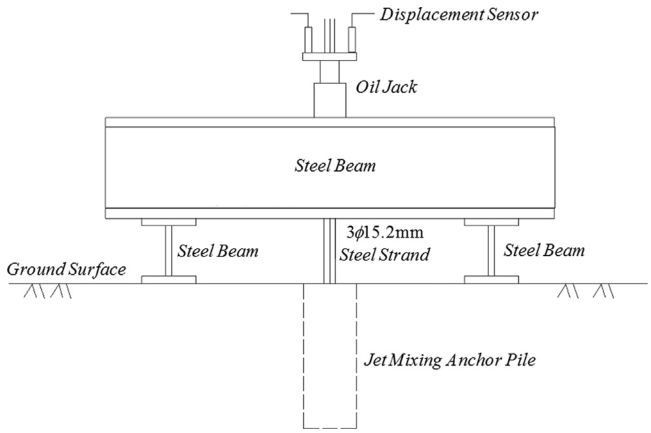

Fig. 2. Schematic diagram of the test equipment.

Fig. 3. Photo of the tests.

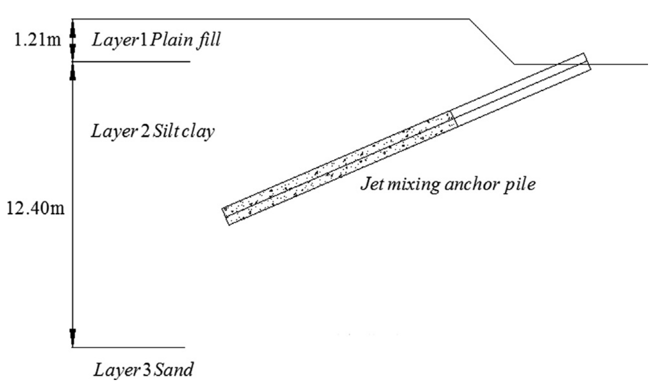

Fig. 4. The foundation soil profile.

Table 2
Parameters of the foundation soil.

Layer	Depth (m)	Unit weight (kN/m^3)	Cohesion (kPa)	Friction angle (°)	Young's modulus (MPa)	Ultimate side friction (kPa)
1	1.21	18.0	10	15	9	12
2	12.40	17.7	12	13	15	22
3	1.30	18.0	7	27	18	70

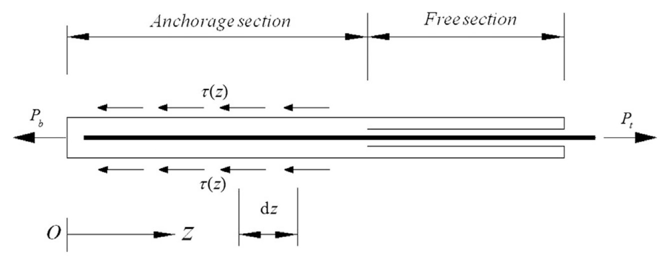

Fig. 5. Calculation model of a single pile.

to supporting structures in silt clays and has good prospects in engineering application.

4. Load-transfer analysis of the piles

So far no theoretical load–deformation analysis has been set up on jet mixing anchor piles. The load-transfer method widely used in the analysis of compression piles and normal anchors is applied to the study in this paper. Ever since the load-transfer method was established by Seed and Reese, many researchers have proven the feasibility and rationality of their method and set up several relative load-transfer functions. Some common functions are the ideal elastic-plastic model (Kim, 2003), the bilinear hardening model(Mayoral et al., 2010), the hyperbolic model (Hirayama, 1990), the parabolic model (Li et al., 2012) and the exponential function model (Zhang and Wang, 2007). It has been proved by theories and practices that the hyperbolic model is more suitable for piles under uplift load.

A single test pile is composed of the free section and the anchorage section, as can be seen in Fig. 5. The free section is also grouted, but the steel strand is not bonded with the cemented soil, so the axial force of the steel strand along the free section is equal to the tension load at the top of the pile. The tension deformation of the free section can be calculated as,

$$S_f = P_t l_f / E_s A_s \tag{1}$$

where, S_f and l_f are the deformation and length of the free section. P_t is the tension load at the top of the pile. E_s and A_s are the elastic modulus and area of the steel strand.

The tension load at the top of the anchorage section is also equal to P_t. The load-transfer relationship between the anchorage section and the surrounding soil can be expressed by the following function, also see the hyperbolic curve in Fig. 6.

$$\tau(z) = w(z)/[a + bw(z)] \tag{2}$$

where, $\tau(z)$ is the shear stress at the position of z. $w(z)$ is the relative displacement between pile and soil at z. The reciprocal of a is the initial tangent slope of the hyperbolic curve. The reciprocal of b is the asymptotic value of the hyperbolic curve, which is also close to the ultimate frictional force of the soil. Both a and b have been endowed with definite

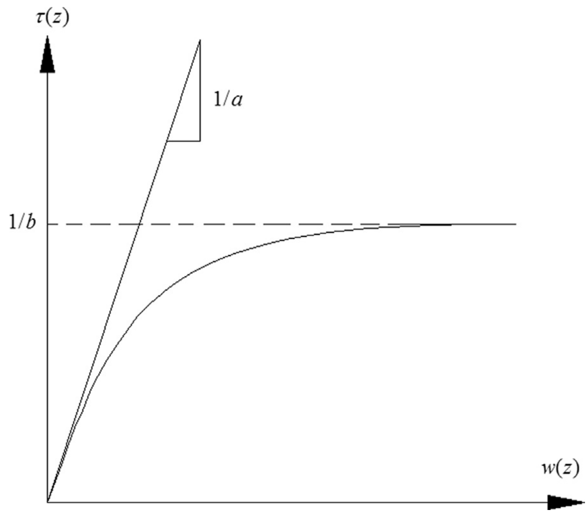

Fig. 6. The hyperbolic load-transfer model.

physical meaning (O'Neill and Hassan, 1994; Sooil, et al., 1999), see function (3).

$$a=\frac{2D}{E_s},\ b=\frac{1}{f_{\max}} \tag{3}$$

where, D is the diameter of the pile. E_s is the Young's modulus of the foundation soil. $f_{\max}$ is the ultimate frictional force of the soil.

Though it is not as easy to test Young's Modulus of the soil directly as it is to test many other modulus in soil, Young's Modulus has some relationship with the compression modulus, and the compression modulus E_c can be achieved by a compression test under lateral restraint. Yang gave the relationship between E_s and E_c for soft clay: $E_s=(2.5–3.5)E_c$ (Yang and Zhao, 1992). The E_c of the second layer of soil is 5 MPa by compression test, and we set 15 MPa as its Young's Modulus in the later calculation.

The side friction can be calculated with Hong's function: (Hong, 1995)

$$\tau_j=c_j+k_{0j}\left(\sum_{i=1}^{j-1}\gamma_i h_i+\frac{1}{2}\gamma_j h_j\right)\tan\,\phi_j \tag{4}$$

where, τ_j is the side friction, c_j and ϕ_j are the cohesion and friction angle which also can be get from the table in M4, $k_{0j}=1-\sin\phi_j$, $\gamma_i h_i$ is the product of the depth of each layer and its unit weight. It should be pointed out that since the bottom of the pile did not reach the bottom of the second layer, the depth of the soil should be carefully evaluated according to the real situation. In this case, for the second layer of the foundation soil, the side friction is 22 MPa.

A typical unit segment of the pile is shown in Fig. 7. It shows that the difference of axial force is equal to the side friction around the unit section. Regardless of the deadweight of the pile, the balance equation of the stress condition of the unit segment can be expressed as,

$$\mathrm{d}P(z)/dz=u\tau(z) \tag{5}$$

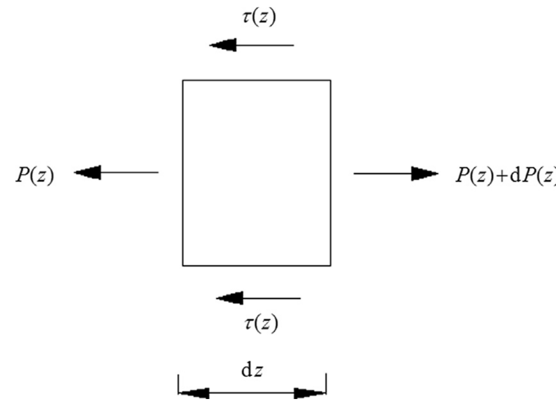

Fig. 7. Stress condition of a unit segment.

where, u and $P(z)$ are the perimeter and axial force of the segment. The stress–strain relationship of the segment is,

$$\mathrm{d}w(z)/\mathrm{d}z=P(z)/EA \tag{6}$$

where, E and A are the elastic modulus and area of the anchorage section. If we combine functions (5) and (6), we can get,

$$\frac{\mathrm{d}P(z)}{\mathrm{d}w(z)}=\frac{uEA}{P(z)}\tau(z) \tag{7}$$

Take function (2) into (7),

$$P(z)\mathrm{d}P(z)=EAu\frac{w(z)}{a+bw(z)}\mathrm{d}w(z) \tag{8}$$

Integrate function (8),

$$P(z)=\frac{\sqrt{2EAu}}{b}\sqrt{bw(z)-a\ln\left(1+\frac{b}{a}w(z)\right)+c_1} \tag{9}$$

where, c_1 is a constant. Considering the boundary condition that $P(z)|_{z=0}=P_b$, $w(z)|_{z=0}=w_b$, where, P_b and W_b are the axial force and displacement at the bottom of the anchorage section, one gets,

$$P(z)=\sqrt{P_b^2+\frac{2EAu}{b^2}\left\{b(w(z)-w_b)-a\ln\left[1+\frac{b(w(z)-w_b)}{a+bw_b}\right]\right\}} \tag{10}$$

c_1 is solved in function (10). Take function (10) into (6),

$$\mathrm{d}z=\frac{EA}{\sqrt{P_b^2+\frac{2EAu}{b^2}\left\{b(w(z)-w_b)-a\ln\left[1+((b(w(z)-w_b))/(a+bw_b))\right]\right\}}}\mathrm{d}w(z) \tag{11}$$

Integrate function (11)

$$z=\int_{w_b}^{w(z)}\frac{EA}{\sqrt{P_b^2+(2EAu/b^2)\{b(w(z)-w_b)-a\ln[1+((b(w(z)-w_b))/(a+bw_b))]\}}}\mathrm{d}w(z) \tag{12}$$

The load–displacement relationship of the pile at any position z can be solved with functions (10) and (12). For a pullout pile, the stress at the bottom, P_b, can be assumed to be zero. Given that the displacement at the bottom of the pile W_b is from zero to a certain value such as 0.1 mm, 1 mm, 10 mm,

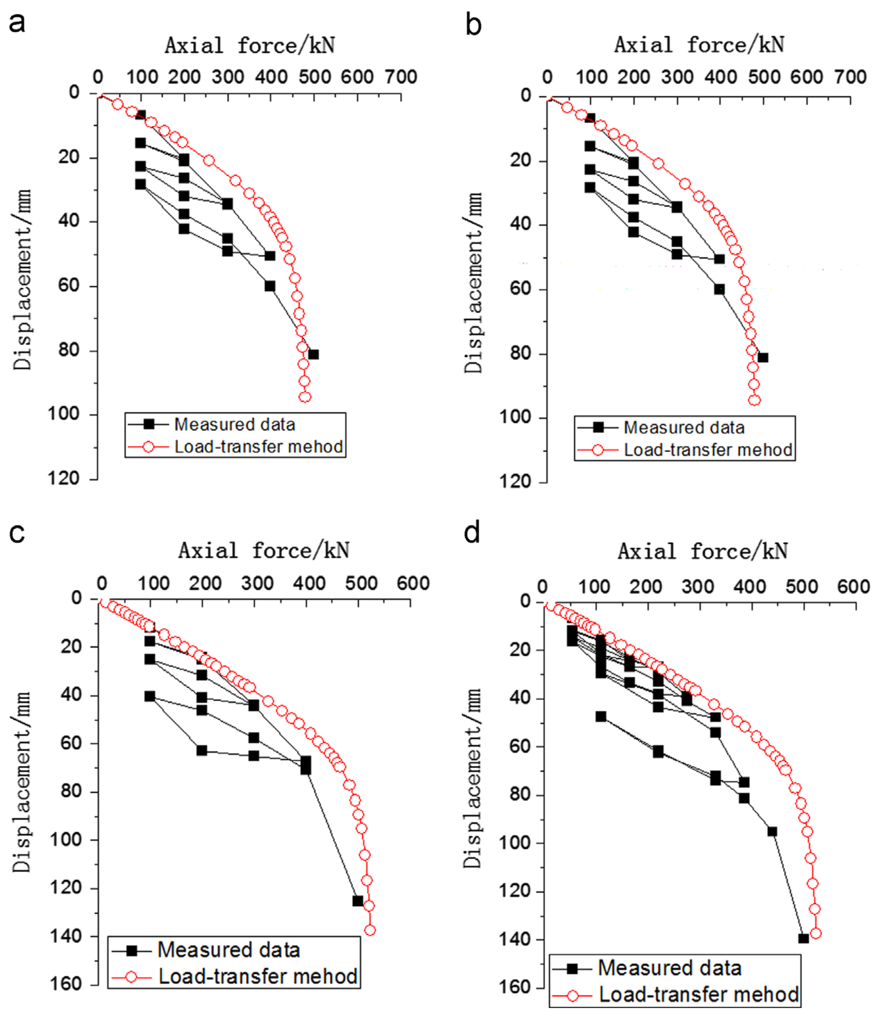

Fig. 8. Comparison between the calculated and measured results of the uplift tests. [(a) Group 1 pile 1, (b) Group 1 pile 2, (c) Group 2 pile 1, (d) Group 2 pile 2].

etc. For each position z, the integral upper limit of function (12) is the displacement of the pile at z. The integral upper limit will be the displacement of the top of the anchorage section when z is equal to the length of the anchorage section. The axial force at the top of the anchorage section can be obtained with function (10). Thus, one can get the relationship between the displacement S_a and the load P_t at the top of the anchorage section with a given series of W_b. Combining function (1), the load–displacement relationship of the whole pile is,

$$S = S_a + P_t l_f / E_s A_s \tag{13}$$

For the test piles in Jingjiang, according to function (3), $1/a = 10\ \text{MN/m}^3$, $1/b = 22$ kPa. The elastic modulus of the grout and the steel bars are 300 MPa and 210 GPa. A comparison between the calculated and measured load–displacement curve is shown in Fig. 8. Fig. 8 also shows the comparison between the calculated and measured results of the uplift tests of single piles. The solid black line represents the measured load–unload displacement relationship of the in-situ tests. The hollow red line represents the calculated load–displacement relationship with the load-transfer method. The good agreement between the two lines proves the accuracy of the proposed load-transfer method. We also can find the elastic-plastic inflection point in Fig. 8a: the inflection point is about 400 kN in axial force. The bearing capacity of the single pile can be decided using this inflexion point.

We can also conclude from the above derivation progress that if the uplift force on the top of the pile is small, the side friction around the upper part of the pile can offset the uplift force and there will be no side friction on the lower part of the pile, as shown in Fig. 9. With the growth of the uplift force, the side friction transfers to the lower part. If the side friction reaches its limit at the top of the pile, it will no longer increase, but the side friction on the lower part of the pile will continue to increase, and then reach its limit again. This indicates that the region where side friction reaches the limit is the failure zone, as can be seen in Fig. 9.

It is a coincidence that the test piles are all in the second layer of the foundation soil. A weighted average parameter is often used to define a layer in scientific research and practical engineering. If a pile passes through several layers, it can also be solved by the proposed method in this manuscript. First, divide the pile into n sections according to the layers, $n = 1,2,3\ldots$, and the NO n section is the lowest section at the bottom of the pile. One can achieve displacement at the top of

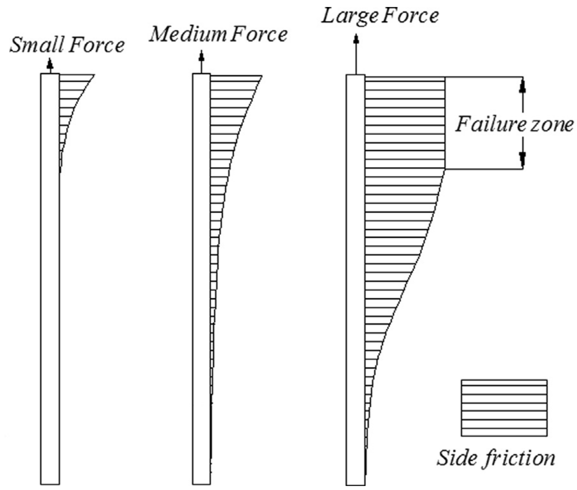

Fig. 9. Load transfer and failure zone of the pile–soil interaction.

section n with the proposed method and the soil parameters of layer n. This displacement is also the displacement at the bottom of section $n-1$, and then with the soil parameters of layer $n-1$, the displacement at the top of section $n-1$ can be solved, and the calculations can be continued in this manner. The displacement at the top of the pile can be finally solved, which will also be the displacement of the pile head. Similar derivations may be applied to belled piles (Honda et al., 2011).

5. Influence scope of the piles

The arrangement of the transverse and vertical spacing of the piles is very important in practical engineering. A single pile from the pile group never behaves the same as an isolated pile. The tension force transferred from the pile into the soil will cause stress overlapping in the soil. The frictional resistance between the anchorage section and soil is reduced by this kind of mutual interference. This phenomenon is called the pile group effect or the anchor group effect (Lee et al., 2002; Vanitha et al., 2007).

It has been derived that the displacement of the anchorage section is $W_c(z)$ under the tension load P_t. The displacement of the soil surrounding the pile is $W_s(z,r)$, where, r is the radial distance from the center of the pile. It is obvious that the deformation of the soil is related to both z and r. Considering that $W_s(z,r)$ decrease with the increase of r and approach zero if r is large enough, the expression of $W_s(z,r)$ can be in the following form, also see Fig. 10.

$$W_s(z,r) = W_c(z) - r \Big/ \left[\alpha - \frac{1}{W_c(z)} r\right] \tag{14}$$

The deformation curve of function (14) is a modified function of Alamgir's expression (Alamgir et al., 1996) according to the boundary conditions of the actual soil situation. The decay rate of the function curve is decided by the unique parameter α. Accurate soil deformation form can be obtained if α is correctly valued.

The pile is divided into n segments vertically. The surrounding soil is correspondingly divided into n blocks vertically and

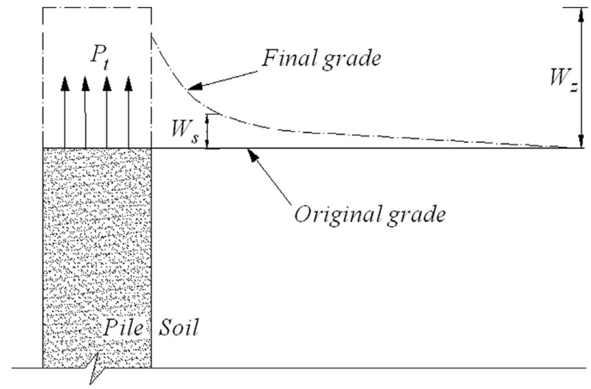

Fig. 10. Deformation of the pile and the surrounding soil.

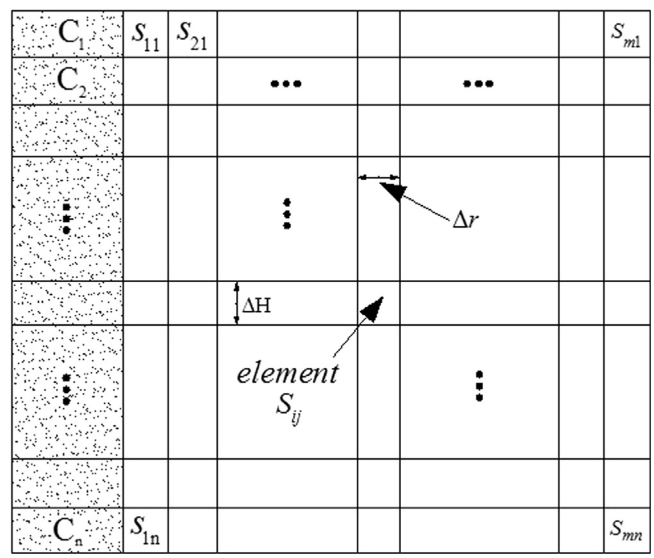

Fig. 11. Pile and soil blocks.

m blocks transversely, see Fig. 11. Function (14) is changed into,

$$W_{sij} = W_{cj} - r/[\alpha_j - r/W_{cj}] \tag{15}$$

The shear strain of the surrounding soil is,

$$\gamma_{sij} = \partial W_{sij}/\partial r = -\left[\frac{1}{\alpha_j + r/W_{cj}} - \frac{r/W_{cj}}{(\alpha_j + r/W_{cj})^2}\right] \tag{16}$$

and the shear stress is,

$$\tau_{sij} = \gamma_{sij} \cdot G_s = -G_s\left[\frac{1}{\alpha_j + r/W_{cj}} - \frac{r/W_{cj}}{(\alpha_j + r/W_{cj})^2}\right] \tag{17}$$

where, G_s is the shear modulus of the soil. The calculated result of function (17) will be equal in value and opposite in direction to the shear stress along the pile if the value of r is the same to the radius of the pile. With the former proposed load-transfer method, W_{cj} can be obtained by function (12) and the shear stress along the pile can be obtained by function (2). Thus, α_j can be derived with a simple computer program. The deformation and shear stress of the soil can be calculated with functions (15) and (17) subsequently. For the former test piles, the decay curve of shear stress in the radial direction of soil at

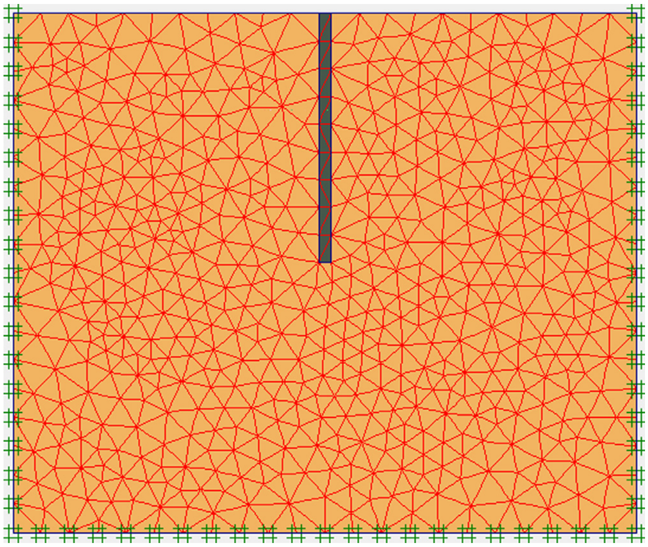

Fig. 12. Elements of the model.

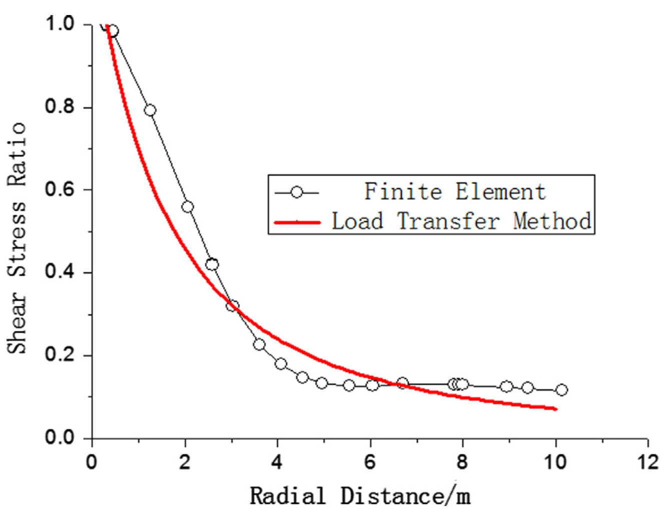

Fig. 13. Shear stress comparison of the two methods.

the ground surface is shown in Fig. 13, where the vertical axis is the ratio between shear stress of soil and along the pile.

The unique parameter α_j of function (14) is obtained through an accurate calculation with the load-transfer method, which means the proposed derivation of the decay curve is credible. It can be concluded from Fig. 13 that the shear stress ratio is reduced to 40% as r reaches 2 m. Engineers can use the percentage as a standard to decide the space needed between any two anchor piles. The engineering significance of the proposed method is that the minimum transverse spacing of jet mixing anchor piles of a project can be calculated simply by applying the load-transfer method.

A finite element model is set up to confirm the rationality of function (14). To date there has been no precedent test of soil displacement of any compression pile or uplift pile (Dash and Pise, 2011; Amit and Nihar, 2009; Nanda and Patra, 2011). This explains the comparison Alamgir made with finite element method results (Alamgir et al., 1996). The finite element method was carried out by the Plaxis software, and all the value of the

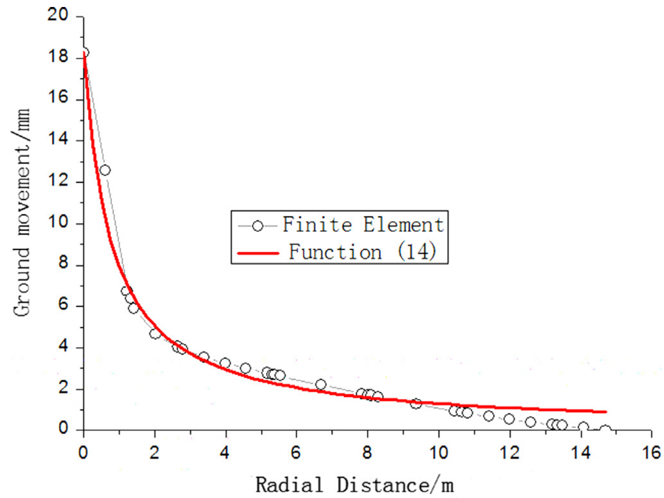

Fig. 14. The fitting results of ground movement.

parameters of the model are the same to the uplift tests, as shown in Table 2. The depth of the model was twice that of the anchor pile, and the radial distance was 20 times of the diameter of the pile, as is the case in the standard models most current researchers use (Said et al., 2009; Dijkstra et al., 2011).

The finite element model is only at the anchorage part of the pile, but the length of the pile is 12 m and the diameter is still 0.6 m. Since the size of each element is set as 0.1 m, there are a total of about 36,000 elements. The software is not capable of producing output for all of these elements. Detailed elements are shown in Fig. 12. The bottom and both sides of the model are fixed. The pile itself is elastic and the soil is elastic and Mohr Coulomb is plastic. The shear strength parameter can be taken from Table 2 in the manuscript.

The finite element results are in good agreement with those of the load-transfer method in terms of decreasing the shear stress ratio, as shown in Fig. 13. The little panes in Fig. 14 are the calculation results of the finite element method, indicating a decrease in the vertical ground movement of the soil with the radial distance to the center of the pile. A red function line (14) was used to fit the ground movements, indicating that agreement is satisfactory, which proves that function (14) is suitable for the expression of vertical ground movement.

6. Conclusion

A new kind of supporting structure for excavation engineering and slope engineering called the jet mixing anchor pile is introduced in this paper. Along with the uplift tests, the load-transfer method is applied to study the tension load–displacement relationship and ultimate bearing capacity of a single pile. The calculated deformations were in close agreement with those of the pullout tests, which proves the accuracy and applicability of the proposed method. The decay mode of shear stress of the surrounding soil is derived based on the load-transfer method, which can be used to decide the minimum transverse spacing of piles in practical engineering.

Acknowledgments

The financial aid of the study reported herein are Project (51178267) supported by the National Natural Science Foundation of China and Project (10231200600) supported by the Science and Technology Committee of Shanghai.

References

Alamgir, M., Miura, N., Poorooshasb, H.B., Madhav, M.R., 1996. Deformation analysis of soft ground reinforced by columnar inclusions. Comput. Geotech. 18 (4), 267–290.

Amit, S., Nihar, R.P., 2009. Effect of arching on uplift capacity of single piles. Geotech. Geol. Eng. 27, 365–377.

Cem, A., Mustafa, K., 2012. Axial bearing capacity of socketed single cast-in-place piles. Soil Found. 52 (1), 59–68.

Dash, B.K., Pise, P.J., 2011. Effect of Compressive Load on Uplift Capacity of Model Piles. J. Geotech. Geo-environ. Eng. 129 (11), 987–992.

Dijkstra, J., Broere, W., Heeres, O.M., 2011. Numerical simulation of pile installation. Comput. Geotech. 38 (5), 612–622.

Hirayama, H., 1990. Load-settlement analysis for bored piles using hyperbolic transfer functions. Soils Found. 30 (1), 55–64.

Hong, Y.K., 1995. Soil Property and Soil Mechanics. China communication press (in Chinese), Beijing, China.

Honda, T., Hirai, Y., Sato, E., 2011. Uplift capacity of belled and multi-belled piles in dense sand. Soil Found. 51 (3), 483–496.

Kiyoshi, Y., Takeshi, Y., Junji, H., 2011. Investigation of settlement and load sharing on piled rafts by monitoring full-scale structures. Soil Found. 51 (3), 513–532.

Kim, N.K., 2003. Performance of Tension and Compression Anchors in weathered soil. J. Geotech. Geo-environ. Eng. 129 (12), 1138–1150.

Liu, Q.L., 2011. Supporting mechanism and stiffness of jet grouting mixing stiffening piles in foundation pits in soft clay. Chin. J. Geotech. Eng. 33 (Suppl. 1), S339–S343 (in Chinese).

Li, X.B., Wei, J., Li, Y.P., Zhu, B., 2012. Normalized numerical analysis for load–displacement curve of uplift pile in soft soil. Adv. Mater. Res. 446, 1462–1467.

Lee, C.J., Bolton, M.D., Al-Tabbaa, A., 2002. Numerical modelling of group effects on the distribution of dragloads in pile foundations. Geotechnique 52 (5), 325–335.

Miyata, Y., Richard, J.B., Takeharu, K., 2009. Measured and predicted loads in multi-anchor reinforced soil walls in Japan. Soils Found. 49 (1), 1–10.

Mayoral, J., Mendoza, M., Flores, F., Romo, M., Ibarra, E., 2010. Modeling soil-pile interaction under axial loading using a bilinear Mohr–Coulomb based model. GeoFlorida 2010, 204–213.

Nanda, S., Patra, N.R., 2011. Shaft resistance of piles in normally consolidating marine clay subjected to compressive and uplift load. In: Proceedings of the Geo-Frontiers 2011, pp. 263–272.

O'Neill, M.W., Hassan, K.M., 1994. Drilled shafts: effects of construction on performance and design criteria. Proc. Int. Conf. Des. Constr. Deep Found. 1, 137–187.

Pastaskorn, K., Tatsunori, M., Ryuuichi, S., 2011. Approximate numerical analysis of a large piled raft foundation. Soil Found. 51 (1), 1–10.

Richard, J.B., Miyata, Y., Takeharu, K., 2011. Limit states design calibration for internal stability of multi-anchor walls. Soil Found. 51 (6), 1051–1064.

Reddy, E.S., O'Reilly, M., Chapman, D.N., 1998. Modified T-Z model – a software for tension piles. Comput. Struct. 68 (6), 653–658.

Shubhra, G., Nihar, R.P., 2007. Prediction of load displacement response of single piles under uplift load. Geotech. Geol. Eng. 25, 57–64.

Sooil, K., Sangseom, J., Sunghan, C., Innjoon, P., 1999. Shear load transfer characteristics of drilled shafts in weathered rocks. J. Geotech. Geo-environ. Eng. 125 (11), 999–1010.

Said, I., Gennaro, V.D., Frank, R., 2009. Axisymmetric finite element analysis of pile loading tests. Comput. Geotech. 36 (1–2), 6–19.

Vanitha, L., Patra, N.R., Chandar, S., 2007. Uplift capacity of pile group anchors. Geotech. Geol. Eng. 25, 339–347.

Yang, M., Zhao, X.H., 1992. Analysis of single pile in layered soil. J. Tongji Univ. 20 (4), 421–428 (in Chinese).

Zhang, L., Wang, H., 2007. Development of residual forces in long driven piles in weathered soils. J. Geotech. Geo-environ. Eng. 133 (10), 1216–1228.